An Electronically Active Molecularly Doped Polyimide Hole Injection Layer for an Efficient Hybrid Organic Light-Emitting Device

Youngkyoo Kim*

Department of Physics, Blackett Laboratory, Imperial College London, Prince Consort Road, London SW7 2BW, United Kingdom

Kwan Hoo Bae, Young Yi Jeong, and Dong Kwon Choi

Institute for Advanced Engineering, Yongin P.O. Box 25, Kyounggi-Do 449-860, Republic of Korea

Chang-Sik Ha

Department of Polymer Science and Engineering, Pusan National University, Pusan 609-735, Republic of Korea

Received May 19, 2004. Revised Manuscript Received August 5, 2004

An efficient hybrid organic light-emitting device (HOLED) has been fabricated with an electronically active molecularly doped polyimide (AMDPI) thin film as a hole injection layer. The AMDPI thin film was prepared by the mixed vapor deposition polymerization process using *N*,*N*′-diphenyl-*N*,*N*′-bis(1-naphthyl)-1,1′-biphenyl-4,4′-diamine, pyromellitic dianhydride, and *N*,*N*′-diphenyl-*N*,*N*′-bis(4-aminobiphenyl)-1,1′-biphenyl-4,4′-diamine that was chemically reduced from its nitro compound synthesized by the coupling reaction in the presence of a polar palladium organometallic catalyst. The ionization potential of the AMDPI thin film was almost similar to that of the undoped polyimide (5.1 eV). The actual contact barrier height between the ITO electrode and the polyimide hole injection layer was approximately 0.2 eV, which is slightly lower than the value (0.4 eV) calculated on the basis of the flat energy band diagram. The HOLED with the AMDPI thin film as a hole injection layer exhibited a maximum performance of ∼80 000 cd/m^2 and ∼7 cd/A. In particular, this HOLED showed quite lower leakage current compared to the OLED with small molecules at the same thickness of hole injection layer, while a much improved device lifetime was measured for the HOLED.

Introduction

Since the encouraging breakthroughs in organic light-emitting devices (OLEDs) based on organic small molecules and polymers, significant progress has been made in the viewpoint of research as well as products.[1−3] However, when it comes to display products with fine pixels on a scale of several micrometers, not just test devices, there is still a controversy on the reliability of the OLED based on small molecules. This is why the lifetime requirements of the products in the marketplace such as car audio and cell phone displays were not completely satisfactory for electronic device applications at an elevated temperature higher than 85 °C. One of the major causes responsible for this poor reliability at high temperature is the imperfect thin film formation leading to progressive electrical shorts, low impact strength, and poor dimensional stability, because a weak van der Waals force is a main means for binding individual small molecules in thin film geometry.[4]

One of the alternative approaches to overcome this problem is the application of polymeric thin films for a hole injection layer (HIL) or a hole transport layer (HTL), where the first organic layer contacts an anode while other layers including an emission layer (EML) consist of small molecules, because polymers can easily form thin films and exhibit high dimensional stability in thin films.[5] This family of OLED can be classified as a hybrid OLED (HOLED).[6,7] Of several types of polymers used for HOLED, an electronically active polyimide has been regarded as one of the most promising polymers for HIL or HTL since polyimide thin films are still being used as dielectric interlayers or packaging layers in microelectronic devices due to their outstand-

* Corresponding author. Tel: +44-020-759-47562. Fax: +44-020-758-13817. E-mail: y.kim@ic.ac.uk.

(1) Tang, C. W.; VanSlyke, S. A. *Appl. Phys. Lett*. **1987**, *51*, 913.
(2) Burroughes, H.; Bradley, D. D. C.; Brown, A. R.; Marks, R. N.; Mackay, K.; Friend, R. H.; Burn, P. L.; Holmes, A. B. *Nature* **1990**, *347*, 539.
(3) Mahon, J. K. *SID Digest* **2001**, 22.
(4) Kim, Y.; Choi, D. K.; Lim, H.; Ha, C. S. *Appl. Phys. Lett*. **2003**, *82*, 2200.
(5) Kim, Y.; Keum, J.; Lee, J. G.; Lim, H.; Ha, C. S. *Adv. Mater. Opt. Electron*. **2000**, *10*, 273 and references therein.
(6) Kim, Y.; Jeong, Y. Y.; Choi, D. K. *IEEE J. Quantum Electron*. **2002**, *38*, 1039.
(7) Kim, Y.; Han, K.; Ha, C. S. *Macromolecules* **2002**, *35*, 8759.

10.1021/cm049200q CCC: $27.50
Published on Web 10/27/2004

ing physical, chemical, and thermal properties as well as the excellent thin film formation and planarization characteristics.[8] Another particular point of polyimide is that it is one of few polymers that can be formed into thin films from its monomers by dry processes in a vacuum such as physical and chemical vapor deposition polymerizations (VDP).

Considering the easy control of polymeric thin film thickness and compositions by deposition speed manipulation in a vacuum, the mixed VDP (MVDP) process has been examined for the fabrication of molecularly doped polyimide (MDPI) thin films for a HIL or a HTL and an EML, in which an insulating polyimide was used to bind electronically active small molecules.[9,10] Although these reports proved that the HOLED fabricated by the VDP process of a hole-transporting polyimide is more thermally stable than the OLED with only small molecules,[6,7,11] the device performance still lagged behind the product level for passive or active matrix displays.[12]

In this work, we have fabricated efficient HOLEDs by using the electronically active MDPI (AMDPI) thin film as a HIL. The AMDPI thin film was prepared by the MVDP process using *N*,*N*′-diphenyl-*N*,*N*′-bis(1-naphthyl)-1,1′-biphenyl-4,4′-diamine (NPB), pyromellitic dianhydride (PMDA), and *N*,*N*′-diphenyl-*N*,*N*′-bis(4-aminobiphenyl)-1,1′-biphenyl-4,4′-diamine (DBABBD) that was chemically reduced with palladium/activated carbon catalyst from its nitro compound synthesized via a polar palladium organometalllic complex catalyst. Considering the energy band structure of the AMDPI thin film, the HTL (NPB) was inserted between the AMDPI thin film and the EML to help better hole injection to the EML. As a result, this HOLED showed a high luminance of ~80 000 cd/m^2 and maximum efficiency of ~7 cd/A. In particular, the leakage-related base current of the HOLED was quite lower than that of the OLED with only small molecules at the same HIL thickness, indicative of the better molecular packing property of the AMDPI film than the small molecule film.

Experimental Section

Prior to the device fabrication, we had attempted a new synthetic method different from that in our previous report[7] to examine the possibility of large scale synthesis. This features the application of a polar palladium based organometallic catalyst system[13−15] for the synthesis of *N*,*N*′-diphenyl-*N*,*N*′-bis(4-nitrobiphenyl)-1,1′-biphenyl-4,4′-diamine (DBNBBD) and palladium charcoal based hydrogenation[16] for the chemical reduction of DBNBBD to DBABBD. The synthetic route is shown in Figure 1.

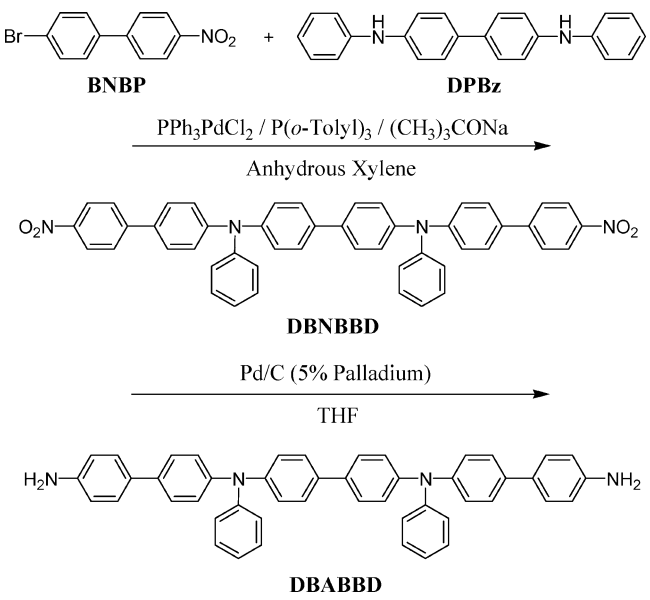

Figure 1. Palladium-mediated reduction of DBABBD from its nitro compound (DBNBBD) synthesized via a polar palladium complex catalyst.

Synthesis of DBNBBD via Polar Palladium Organometallic Catalyst. A mixture solution including 73.6 mL of anhydrous xylene, 18.2 g of 4-bromo-4′-nitrobiphenyl (BNBP), 10 g of *N*,*N*′-diphenylbenzidine (DPBz), 1.04 g of bis(triphenylphosphine)palladium dichloride (PPh_3PdCl_2), and 1.81 g of tri-*o*-tolylphosphine (P(*o*-tolyl)$_3$) was prepared in a glovebox charged with a nitrogen gas to prevent the monomers from oxidation. After vigorous stirring leading to a uniform solution, 7.53 g of sodium-*t*-butoxide was slowly added to the solution. Then the solution filled with all starting materials was heated to 120 °C and kept for several hours. The reaction progress was checked by thin-layer chromatography (TLC). When there was no more change in the TLC spots corresponding to the starting and product materials, the reaction was terminated by cooling the reaction mixture to room temperature. The estimated reaction time was about 12 h. After 200 mL of chloroform was poured into the reaction mixture, the precipitates including the catalysts were removed by filtration and followed by evaporating the chloroform residues in the chloroform/xylene mixture containing the product materials. The solidification of the products was performed by the precipitation of the chloroform-free xylene mixture into an excess of *n*-hexane. These solids were dissolved in an excess of chloroform to be purified by column chromatography. Finally, the hot filtration in methanol led to the desired compound (DBNBBD). The weight and apparent color were 12.4 g and reddish, respectively. Yield: 57.4%. ^{1}H NMR (DMSO-d_6): δ 8.26 (d, 4H), 7.92 (d, 4H), 7.74 (d, 4H), 7.63 (d, 4H), 7.38 (t, 4H), 7.15−7.07 (m, 14H). T_g: 130 °C. MS (*m*/*e*): calcd, 730.26 (M^+); found, 730.8 (M^+). Anal. Calcd for $C_{48}H_{34}N_4O_4$: C, 78.89; H, 4.49; N, 7.67; O, 8.76. Found: C, 78.92; H, 4.93; N, 7.58; O, 8.57.

Reduction of DBNBBD to DBABBD via Pd/C Catalyst. A heterogeneous mixture including 3 g of DBNBBD, 0.5 g of 5% palladium on activated carbon (Pd/C), and 100 mL of tetrahydrofuran was loaded on a hydrogenation reactor (Parr Co.). Then the mixture was vigorously shaken with continuous purging of hydrogen gas for 24 h at a pressure of ~43 psi. After termination of the shaking, the reaction mixture was filtered off to remove the Pd/C slurries and other solid impurities and followed by evaporating the tetrahydrofuran solvent by using a rotary evaporator. To separate the reduced product from the crude solids, a silica gel column chromatography was used with

(8) *Polyimides: Fundamentals and Applications*; Gosh, M. K., Mittal, K. L., Eds.; Marcel Dekker: New York, 1996.
(9) Lee, J. G.; Kim, S.; Choi, D. K.; Kim, Y.; Kim, S. C.; Lee, M. H.; Jeong, K. *J. Korean Phys. Soc*. **1999**, *35*, S604.
(10) Wen, W. K.; Jou, J. H.; Chiou, J. F.; Chang, W. P.; Whang, W. T. *Appl. Phys. Lett*. **1997**, *71*, 1302.
(11) Kim, Y.; Lee, J. G.; Han, K.; Hwang, H. K.; Choi, D. K.; Jung, Y. Y.; Keum, J. H.; Kim, S.; Park, S. S.; Im, W. B. *Thin Solid Films* **2000**, *363*, 263.
(12) Wang, Y. F.; Chen, T. M.; Okada, K.; Uekawa, M.; Nakaya, T.; Kitamura, M.; Inoue, H. *J. Polym. Sci.: Part A: Polym. Chem*. **2000**, *38*, 2032.
(13) Louie, J.; Hartwig, J. F. *Tetrahedron Lett*. **1995**, *36*, 3609.
(14) Wolfe, J. P.; Wagaw, S.; Buchwald, S. L. *J. Am. Chem. Soc*. **1996**, *118*, 7215.
(15) Hartwig, J. F.; Richards, S.; Baranano, D.; Paul, F. *J. Am. Chem. Soc*. **1996**, *118*, 3626.
(16) *Organic Syntheses*; Baumgarten, H. E., Ed.; John Wiley & Sons: New York, 1973; Collect. Vol. V, Chapter 5, pp 30−1130.

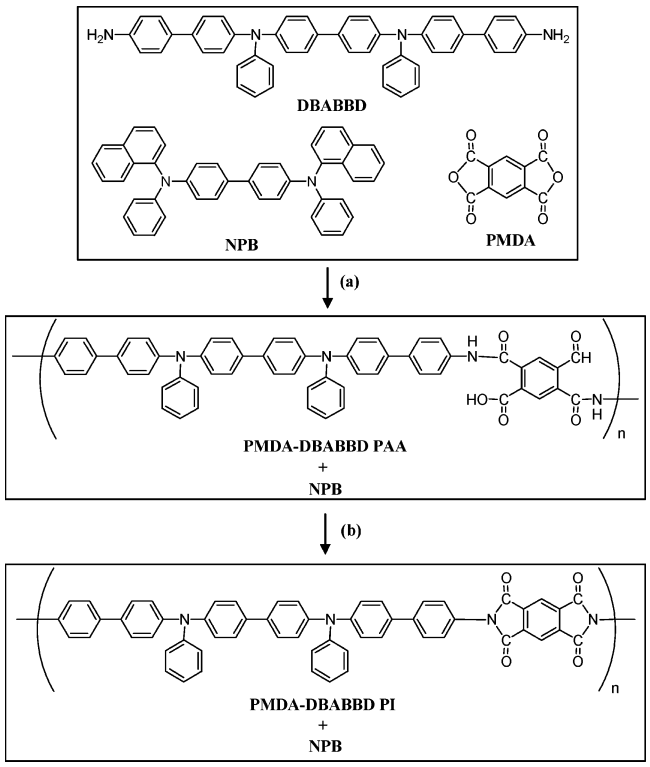

Figure 2. Fabrication of the AMDPI thin film: (a) mixed vapor deposition polymerization process; (b) thermal imidization of precursor composite thin film.

an eluent of chloroform/ethyl alcohol (5/1). After the eluents evaporated, the resulting powders were further precipitated into methanol, leading to 0.51 g of the desired solid product (DBABBD), which was slightly yellowish white. Yield: 18.5%. ^{1}H NMR (DMSO-d_6): δ 7.55 (d, 4H), 7.48 (d, 4H), 7.31−7.28 (m, 8H), 7.07−7.02 (m, 10H), 6.61 (d, 4H), 5.17−5.19 (d, 4H). T_g: 130 °C. MS (*m/e*): calcd, 670.31 (M^+); found, 670.8 (M^+). Anal. Calcd for $C_{48}H_{38}N_4$: C, 85.94; H, 5.71; N, 8.35. Found: C, 86.66; H, 5.83; N, 8.28.

Fabrication of Thin Films and Devices. Poly[*N*,*N*′-diphenyl-*N*,*N*′-bis(4-aminobiphenyl)-1,1′-biphenyl-4,4′-diamine pyromellitamic acid] (PMDA-DBABBD PAA) precursor thin film was in-situ synthesized onto a substrate by coevaporating PMDA and DBABBD powders at a deposition rate of 1 Å/s. This precursor film was converted into poly[*N*,*N*′-diphenyl-*N*,*N*′-bis(4-aminobiphenyl)-1,1′-biphenyl-4,4′-diamine pyromellitimide] (PMDA-DBABBD PI), an electronically active polyimide (API) thin film, by thermal imidization at 200 °C for 2 h. The AMDPI thin film, the mixture of PMDA-DBABBD PI and NPB, was prepared by thermal imidization of the precursor mixture film that was made by coevaporating PMDA, DBABBD, and NPB at deposition rates of 0.5, 0.5, and 1 Å/s, respectively. The resulting API and AMDPI thin films were controlled to ∼190 Å thick. A quartz substrate was used for the optical absorption measurement, while an indium tin oxide (ITO) glass was used for the ionization potential (I_P) measurement and the device fabrication. The schematic procedure of the AMDPI thin film preparation is shown in Figure 2.

Hole-only devices (HOD) were fabricated by depositing an aluminum electrode on top of the API and AMDPI thin films coated on the ITO glass (see Figure 3). Two types of HOLED were fabricated. HOLED-1 consists of an anode, the AMDPI thin film, an EML, an electron transporting layer (ETL), and a cathode, whereas HOLED-2 has an additional NPB layer between the AMDPI thin film and the EML. Consequently, the AMDPI thin film plays a HIL role in HOLED-2, whereas it works as both HIL and HTL in HOLED-1. As a comparative device, a conventional OLED was fabricated using 4,4′,4″-tris-[*N*-(3-methylphenyl)-*N*-phenylamino]triphenylamine (m-MTDATA) instead of the AMDPI thin film. The thickness of the

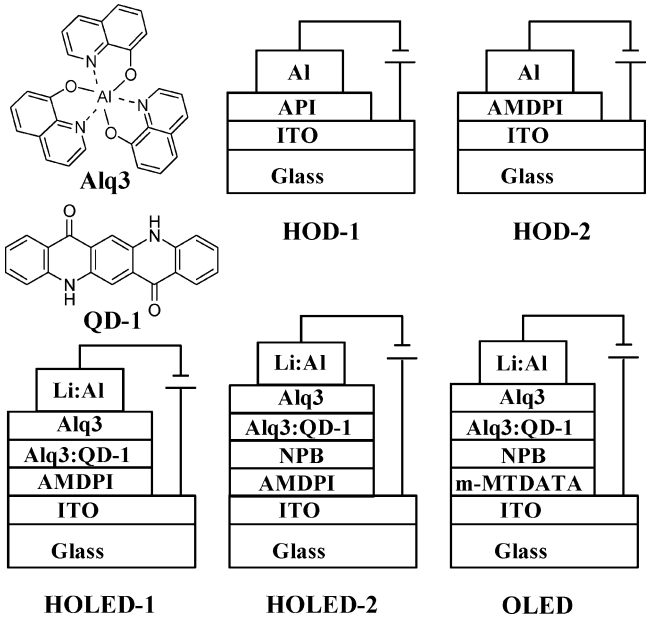

Figure 3. Cross-sectional structure of devices and chemical structure of Alq3 and QD-1.

m-MTDATA and NPB layers was 190 and 50 Å, respectively. The EML was deposited by coevaporating tris(8-hydroxyquinolinato)aluminum (Alq3) and 5,12-dihydroquino[2,3-*b*]acridine-7,14-dione (QD-1) at rates of 2 and 0.02 Å/s, respectively. The ETL (180 Å thick) was prepared by the successive evaporation of the Alq3 molecules after closing a shutter over the crucible containing the QD-1 molecules when the EML reached 150 Å thick. On top of the ETL, the lithium−aluminum alloy (0.1% Li) was evaporated to form a low work function cathode. Finally, all devices were encapsulated with a stainless canister attaching a calcium oxide based desiccant film and UV-curable resins.

Characterization of Materials, Thin Films, and Devices. The synthesized materials were characterized by using a nuclear magnetic resonance spectrometer (Varian Unity Plus 300), a mass spectrometer (Kratos Profile HV-3), an elemental analyzer (Vario EL, Elemental Analyzen Systeme), an infrared spectrometer (Nicolet Protégé 460), and a differential scanning calorimeter (TA Instruments DSC 2910). The optical band gap and ionization potential of the polyimide thin film were measured by using an ultraviolet−visible (UV−vis) absorption spectrometer (Perkin-Elmer Lambda 19) and an ultraviolet photoelectron spectrometer (UPS), respectively. A surface profiler (Tencor P-10) was employed to measure the thin film thickness. The device performance including current−voltage−luminance characteristics and electroluminescent (EL) spectrum was measured by using a system equipped with a source measure unit (Keithley 237) and a candela meter (PR650). Device lifetime of HOLED-2 was measured using a homemade system equipped with a dc current power supply and a calibrated photodiode. The initial luminance was fixed to 500 cd/m^2 while the operation was carried out with dc continuous driving.

Results and Discussion

Characterization of Synthesized Materials. As characterization examples for the synthesized materials compared to the starting ones, the Fourier transform infrared (FT-IR) spectra are shown in Figure 4a. The single N−H stretching band at around 3390 cm^{-1} corresponded to the secondary amine of the DPBz molecule that disappeared after the coupling reaction of DPBz with BNBP molecules. It is considered from the FT-IR spectra of the DBNBBD and DBABBD

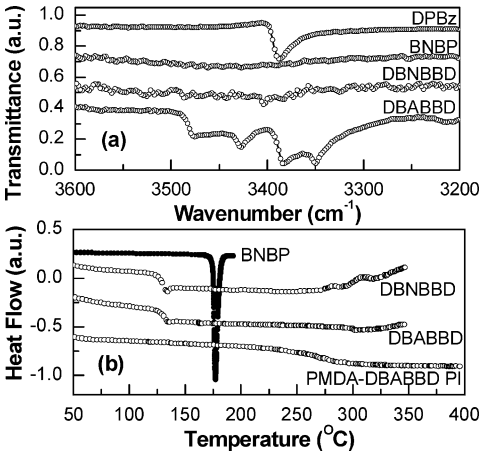

Figure 4. Characterization of synthesized molecules compared to the starting materials by (a) FT-IR and (b) DSC.

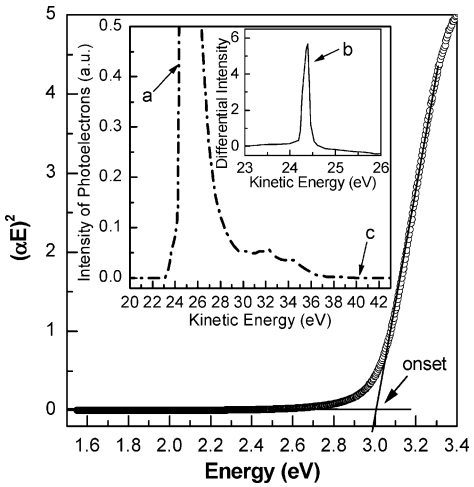

Figure 5. Plot of $(\alpha E)^2$ as a function of photon energy for the AMDPI thin film on a quartz. The inset shows the UPS spectrum and its differential plot of the AMDPI thin film on an ITO glass: (a) Kinetic energy (b) at a maximum differential intensity and (c) Fermi edge.

molecules that the nitro groups of the DBNBBD molecule were successfully reduced into the amino groups of the DBABBD because two distinct bands with a characteristic double peak were observed between 3300 and 3500 cm^{-1}, indicating the formation of a primary amine. However, the phenomenon of the similar peak splitting in the different two bands is not clearly understood at present even though it is generally known that a peak at higher frequency is typically owing to an asymmetric vibration of N−H bond in a primary amine while a symmetric vibration leads to a transmission peak at lower frequency.[17]

Figure 4b shows the DSC thermograms of starting and synthesized materials including the API powder.[7] The glass transition temperature of the DBNBBD and DBABBD powders was approximately 130 °C, whereas no melting point was observed up to 350 °C even though the BNBP powder, one of the reagents, obviously showed a melting point at around 175 °C. From the same glass transition behavior between the DBNBBD and DBABBD powders, it is considered for these kinds of molecules that the nitro and amino groups barely affect the thermal transition of the molecular backbone. It is particularly noteworthy that the glass transition temperature was more than 220 °C for the API powder having the DBABBD and PMDA units in its main chain even though that of the DBABBD powder was only ∼130 °C. Unfortunately, the transition temperature of the AMDPI films could not be measured here because more than 3 mg of powder is typically required for the DSC measurement. However, from the glass transition temperature of the pristine NPB (∼95 °C) and the API powders, that of the AMDPI powder consisting of 50 wt % NPB molecules can be theoretically calculated as ∼148 °C on the basis of the well-known Fox equation.[5]

Energy Band Structure of Thin Films. From the plot of the squared absorption energy variation as a function of photon energy (Figure 5), the band gap of the AMDPI thin film was obtained as ∼3.0 eV, which is slightly wider than the API thin film.[6,7] In the UPS spectrum (inset), the maximum peak value of the differential plot, corresponding to the inflection point of the raw UPS spectrum in a lower kinetic energy region below ∼25 eV, was selected as a cutoff kinetic energy (E_{CF}) that means the highest probability for the existence of photoelectrons with the strongest binding energy to obtain an accurate value without any influence of the retarded or scattered photoelectrons in the lower energy region. From the incident light photon energy (E_{IN}) of 21.2 eV and the kinetic energies for the cutoff (24.39 eV) and the Fermi edge (E_{FE} = 40.39 eV), the I_P of the AMDPI thin film was calculated as ∼5.1 eV using eq 1.[7] This I_P value was confirmed with the conventional analysis method using a gold thin film as a reference.[18] It is interesting that the I_P of the AMDPI film is almost same as that of the API thin film (5.12 eV).[7] On the basis of the I_P and band gap of the AMDPI thin film, its electron affinity was calculated as ∼2.1 eV, in which the binding energy with phonons was not taken into account. Finally, the flat energy band diagrams of devices are constructed in Figure 6.[19]

$$\mathrm{IP} = E_{\mathrm{IN}} - (E_{\mathrm{FE}} - E_{\mathrm{CF}}) \quad (1)$$

It is considered that the lower ionization potentials of the API and AMDPI thin films than those of the very similar pristine small molecule films such as NPB and *N*,*N*′-diphenyl-*N*,*N*′-(3-methylphenyl)-1,1′-biphenyl-4,4′-diamine (TPD) are attributed to the possible activation effect by the interaction between the positive dipole in the carbonyl group of the imide moiety and the lone pair electron in the nitrogen atom of the DBABBD moiety (see Figure 7). Furthermore, in case of the AMDPI thin film, the similar dipole interaction between the nitrogen atom in the NPB molecule and the carbonyl group in the API chain may lead to the almost same ionization potential as the API thin film.

Contact Barrier between Thin Films and ITO. The actual contact barrier height (φ) between the ITO electrode and the API or AMDPI thin film was measured for the hole-only devices using the Fowler−

(17) *Introduction to Spectroscopy: A Guide for Students of Organic Chemistry*; Pavia, D. L., Lampman, G. M., Kriz, G. S., Jr., Eds.; W. B. Saunders Co.: Philadelphia, PA, 1979; Chapter 2, pp 13−80.

(18) Kim, Y.; Im, W. B.; Hwang, H. K.; Lee, J. G.; Han, K.; Kim, S. *Proc. Int. Disp. Manuf. Conf.* **2000**, 431.

(19) Parker, I. D. *J. Appl. Phys*. **1994**, *75*, 1656.

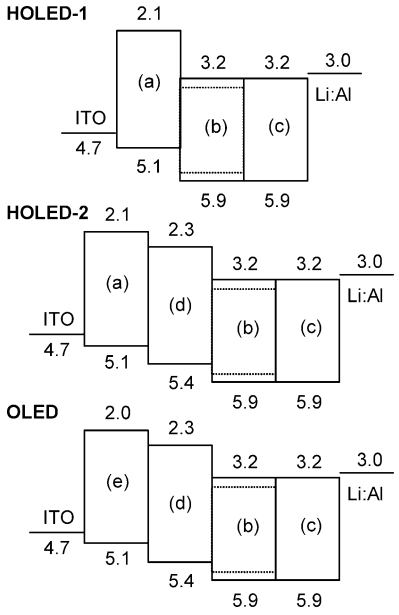

Figure 6. Energy band diagrams of HOLEDs and OLED fabricated in this work.

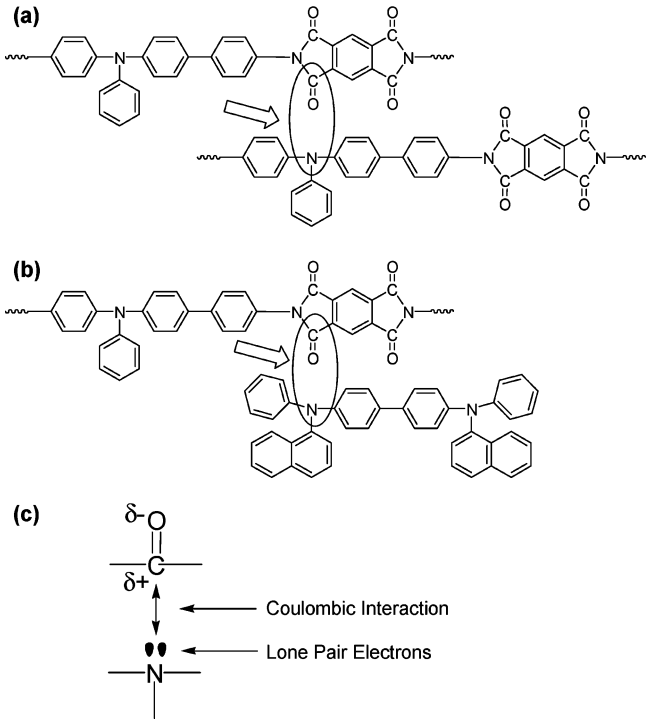

Figure 7. Proposed mechanism for lowering of ionization potential of the AMDPI thin film: (a) interaction between carbonyl moiety and tertiary amine in PMDA-DBABBD PI; (b) interaction between carbonyl moiety in PMDA-DBABBD PI and tertiary amine in NPB molecule; (c) Coulomb interaction between positive dipole in carbonyl group and lone pair electron in nitrogen atom.

Nordheim tunnel injection theory given by the following:[19,20]

$$\ln\left(\frac{J}{F^2}\right) \propto -\frac{8\pi\sqrt{2m^*}}{3qh}\varphi^{3/2}\frac{1}{F} \qquad (2)$$

Here J, F, m^*, and h are the current density, electric field, effective mass of holes, and Planck constant, respectively. From the slope in Figure 8, the barrier

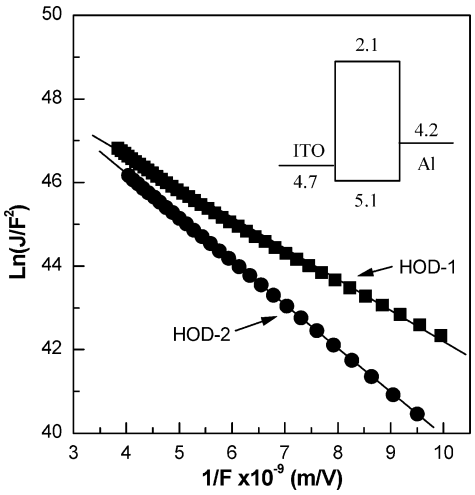

Figure 8. Fowler−Nordheim plot at forward bias and flat energy band diagram (inset) of hole-only devices.

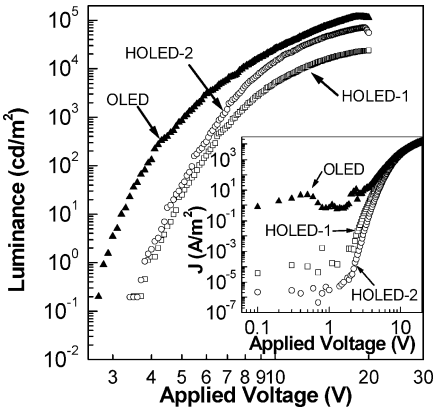

Figure 9. Luminance and current density (inset) characteristics of devices as a function of applied voltage.

height between the ITO electrode and the API thin film (HOD-1) was calculated as ~0.23 eV, whereas that between the ITO and the AMDPI thin film (HOD-2) was ~0.16 eV. Within the experimental error range we can consider these values almost same, so this is in good agreement with the almost identical I_P for the API and AMDPI films from the UPS measurement. It is considered that the energy level alignment at the interface between the ITO and the polyimide thin film is responsible for the slightly reduced actual barrier height compared to the directly calculated value from the work function of the ITO and the I_P of the polyimide film, assuming the same ITO work function.[21]

HOLED Characteristics. At low applied voltage of less than 2 V, the current density of OLED was much higher than that of HOLEDs, indicating that the molecular packing is better for the AMDPI thin film than the small molecule film (m-MTDATA) at the same thickness (see Figure 9). Because the base current was lowered by more than 1 order of magnitude with the addition of HTL in HOLED-2, the NPB molecules in the HTL are considered to play a filler role in healing a possible surface defect such as pinholes and nanovoids. The charge injection was initialized at ~2 V for all the

(20) *Physics of Semiconductor Devices*; Sze, S. M., Ed.; John Wiley & Sons: New York, 1981.
(21) Ishii, H.; Oji, H.; Ito, E.; Hayashi, N.; Yoshimura, D.; Seki, K. *J. Lumin.* **2000**, *87*−*89*, 61 and references therein.

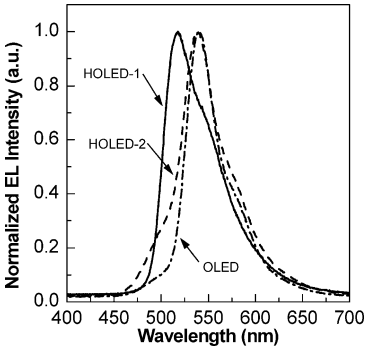

Figure 10. Electroluminescence spectra of devices at 10 V.

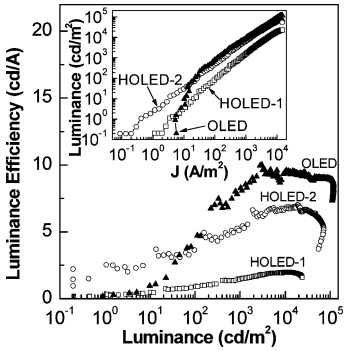

Figure 11. Luminous efficiency and luminance (inset) of devices as a function of luminance and current density, respectively.

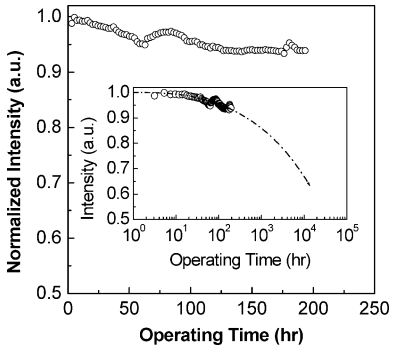

Figure 12. Luminance decay of HOLED-2 as a function of operating time at the initial luminance of 500 cd/m^2 (constant dc driving). The inset shows a semilogarithmic plot with projected lifetime (dash dot line).

devices whereas the turn-on of light occurred at ~2.6, ~3.6, and ~3.5 V for OLED, HOLED-1, and HOLED-2, respectively. The large difference between the turn-on and charge injection voltages indicates that the present HOLEDs were not well balanced compared to the OLED. As the applied voltage increased, HOLED-2 with the AMDPI thin film as a HIL showed a much higher luminance than HOLED-1. From the energy band diagram (Figure 6) it is obvious for HOLED-1 that the hole injection from the AMDPI thin film to the EML is very much limited to supply sufficient hole carriers owing to the large barrier height. The maximum luminance of HOLED-2 reached ~80 000 cd/m^2 while that of OLED was ~120 000 cd/m^2. However, the performance of HOLED-2 can be improved to the level of OLED if the turn-on voltage is further reduced by the optimization of the device structure, because HOLED-2 showed much a stiffer slope for the luminance increase than OLED and HOLED-1.

Another proof for the unbalanced HOLEDs can be observed from the EL spectra in Figure 10. HOLED-2 showed a bigger shoulder at around 480 nm compared to OLED, which is considered as a blue emission from the NPB molecules in the HTL. This indicates the existence of the emission zone close to the interface between HTL and EML. Unlike OLED and HOLED-2, the EL spectrum of HOLED-1 shifted toward higher energy region. This is simply considered as a quite large contribution of the ETL emission because the emission zone can be moved toward the ETL by the slightly higher electric field of HOLED-1 than other devices owing to the thinner EML compared to well-optimized devices.[4] So the EML thickness should be increased to achieve a comparable performance to the well-optimized device.[4]

As the luminance of devices increased, the luminance efficiency increased and then showed a maximum (Figure 11). The maximum luminance efficiency was ~7 cd/A (~2.7 lm/W) and ~9.5 cd/A (~4.9 lm/W) for HOLED-2 and OLED, respectively. In particular, HOLED-2 showed the luminance efficiency of more than 2 cd/A (~1.6 lm/W) at 1 cd/m^2, whereas the luminous efficiency of OLED was very low at the luminance of less than 10 cd/m^2. This is why the leakage current of OLED at low voltage was much higher than HOLEDs at the same HIL thickness (see Figure 9). In addition, the luminance of HOLEDs showed a linear relationship over the entire current density, whereas a nonlinear behavior was observed in OLED in the lower current region. This linear characteristics and low leakage current of HOLEDs may contribute to the further development of organic nanoelectronic devices with ultrathin layers, which need very high rectification and signal-to-noise ratio at quite low voltage.

A preliminary lifetime test was carried out for HOLED-2 at the initial luminance of 500 cd/m^2. Unlike the quick intensity drop of OLED within approximately 200 h,[23] HOLED-2 showed a very slow intensity decrease as shown in Figure 12. The projected lifetime of HOLED-2 is expected to be more than 10 000 h (see inset to Figure 12), even though the reported half-lifetime is only 2500 h at the initial luminance of 300 cd/m^2 for the OLED with Qd-1-doped Alq3 film.[23] It is considered that this improvement is mainly ascribed to the AMDPI thin film because a polymeric layer smoothens the rough ITO surface so that the possibility of electrical shorts can be reduced.[24] In addition, the thermal stabilization of the AMDPI layer during thermal imidization process is considered another reason for the improved lifetime as previously demonstrated for the thermal stability difference between hole-transporting PI and small molecule thin films[11] as well as annealing influence on device lifetime.[4]

Conclusions

The AMDPI thin film exhibiting a theoretical glass transition temperature of ~148 °C was prepared through

(22) Im, W. B.; Hwang, H. K.; Lee, J. G.; Han, K.; Kim, Y. *Appl. Phys. Lett.* **2001**, *79*, 1387.
(23) Wakimoto, T.; Yonemoto, Y.; Funaki, J.; Tsuchida, M.; Murayama, R.; Nakada, H.; Matsumoto, H.; Yamamura, S.; Nomura, M. *Synth. Met.* **1997**, *91*, 15.
(24) Elschner, A.; Bruder, F.; Heuer, H.-W.; Jonas, F.; Karbach, A.; Kirchmeyer, S.; Thurm, S.; Wehrmann, R. *Synth. Met.* **2000**, *111–112*, 139.

the thermal imidization of the precursor mixture film obtained by the MVDP process using NPB, PMDA, and DBABBD that was chemically reduced from its nitro compound synthesized by the coupling reaction in the presence of a polar palladium organometallic catalyst. The ionization potential of the AMDPI thin film was ~5.1 eV, which is almost similar to that of the API thin film. In particular, the base current density of HOLED, directly related to a leakage current of device, was lower by 4−6 orders of magnitude than that of OLED at the same HIL thickness. The maximum luminance of HOLED with the AMDPI thin film as a HIL reached ~80 000 cd/m^2, which is approximately a 74% performance compared to that of OLED. The much improved lifetime of HOLED is likely owing to the thermally stable AMDPI layer. This indicates that the AMDPI thin film is promising for a stable HIL as a contingency of small molecules because it can be fabricated in a vacuum by the same way as small molecule deposition processes.

Acknowledgment. The authors thank Dr. S. Park and Dr. K. Han for helps with material synthesis and film characterization and Prof. K. Jeong at Yonsei University for UPS measurements. Y.K. thanks Prof. D. D. C. Bradley for arranging financial support. Part of this work was financially supported by the National Research Laboratory Program (Korea).

CM049200Q